HHS Public Access

Author manuscript

Proc SPIE Int Soc Opt Eng. Author manuscript; available in PMC 2011 September 18.

Published in final edited form as:

Proc SPIE Int Soc Opt Eng. 2009 February 18; 7162(1): . doi:10.1117/12.816867.

Methods for calculating the severity of demineralization on tooth surfaces from PS-OCT scans

Michael H. Le, **Cynthia L. Darling**, and **Daniel Fried**[1]

University of California, San Francisco, San Francisco, CA 94143-0758

Abstract

Several studies have demonstrated that polarization sensitive optical coherence tomography (PS-OCT) can be used to nondestructively measure the severity of subsurface demineralization in enamel and dentin. The reflectivity in the polarization state orthogonal to the initial linear polarization incident on the tissue is low at sound tissues interfaces and high in demineralized areas that strongly scatter and depolarize the light. The purpose of this study was to develop improved algorithms for assessing the depth and severity of demineralization from PS-OCT scans for use with 2D and 3D tomographic images. Subsurface caries-like lesions of increasing depth and severity were produced in adjoining windows on ten bovine enamel samples by exposure to demineralization over periods of 1 to 4 days. Each sample also had a sound window to be used as a control. PS-OCT scans were acquired for each sample and analyzed using various methods to calculate the lesion depth and area. Algorithms were developed and used to automatically detect the lesion depth and area, and calculate the volume for improved assessment of lesion severity. Both fixed-depth and automatic edge-finding algorithms were able to detect significant differences between each of the days and sound enamel. The lesion depth and mineral loss were also measured with polarized light microscopy and transverse microradiography after sectioning the teeth. Mean lesion depths ranged from 40 to 100 μm. This demonstrates the edge-finding algorithm can be used to automatically determine the depth and severity of early lesions for the rapid analysis of PS-OCT images.

Keywords

Enamel; caries; PS-OCT; image processing algorithms; early demineralization; edge detection

1. INTRODUCTION

New tools are needed to non-destructively assess carious lesion depth and severity, efficacy of chemical intervention, and testing of anti-caries agents. The National Institute of Dental and Craniofacial research has requested the validation of new technologies for the measurement of tooth surface demineralization or remineralization to serve as a likely surrogate end point in dental clinical trials [1]. Several studies have demonstrated that polarization sensitive optical coherence tomography (PS-OCT) can be used to

[1]daniel.fried@ucsf.edu.

nondestructively measure the severity of subsurface demineralization in enamel and dentin and is therefore well suited for this role. Polarization sensitivity is particularly valuable for imaging caries lesions due to the enhanced contrast of caries lesions caused by depolarization of the incident light by the lesion and the confounding influence of the strong surface reflectance of the tooth surface is reduced in the orthogonal polarization. Baumgartner et al. [2–4] presented the first polarization resolved images of dental caries. PS-OCT images are typically processed in the form of phase and intensity images[5,6], such images best show variations in the birefringence of the tissues. Caries lesions rapidly depolarize incident polarized light and the image of the orthogonal polarization to that of the incident polarization can provide improved contrast of caries lesions. We previously developed an approach to quantifying the severity of caries lesion by integrating the reflectivity of the orthogonal axis or perpendicular polarization ($\perp$) [7]. There are two mechanisms in which intensity can arise in the perpendicular axis. The native birefringence of the tooth enamel can rotate the phase angle of the incident light beam between the two orthogonal axes (similar to a wave-plate) as the light propagates through the enamel without changing the degree of polarization. The other mechanism is depolarization from scattering in which the degree of polarization is reduced. It is this latter mechanism that is exploited to measure the severity of demineralization. Complete depolarization of the incident linearly polarized light leads to equal distribution of the intensity in both orthogonal axes. Demineralization of the enamel due to dental decay causes an increase in the scattering coefficient by a 1-2 orders of magnitude [8], thus demineralized enamel induces a very large increase in the reflectivity along with depolarization. This in turn causes a large rise in the perpendicular polarization channel or axis.

This approach also has the added advantage of reducing the intensity of the strong reflection from the tooth surface for measurement of the lesion surface zone that can potentially provide information about the lesion activity and remineralization. A conventional OCT system cannot differentiate the strong reflectance from the tooth surface from increased reflectivity from the lesion itself. The reflectivity in the orthogonal polarization can be directly integrated to quantify the lesion severity, regardless of the tooth topography. By using this approach the difficult task of deconvolving the strong surface reflection from the lesion surface from reflectivity from within the lesion can be circumvented. Longitudinal studies have demonstrated that PS-OCT can be used for monitoring erosion and demineralization. The progression of artificially produced caries lesions in the pit and fissure systems of extracted molars can be monitored non-destructively and the integrated reflectivity in the $\perp$-axis correlates well with the growth of the lesion. Since the most important information about the lesion is near the surface, a polarization sensitive OCT system is invaluable for imaging dental caries particularly early lesions. By exploiting depolarization in the $\perp$-axis of the PS-OCT system we can quantify lesion severity on highly convoluted surfaces.

PS-OCT can rapidly acquire 2D and 3D tomographic images of areas of early demineralization on tooth surfaces. In order to rapidly process the images and effectively quantify the lesion severity algorithms are needed to automatically to extract lesion depth and severity information. This paper will present and evaluate two approaches to automatically assess the depth and severity of demineralized enamel lesions.

2. MATERIALS AND METHODS

2.1 Sample Preparation

Ten enamel blocks, approximately 10 × 3 × 1 mm^3, of bovine enamel were prepared from extracted bovine tooth incisors acquired from a slaughterhouse. Each enamel sample was partitioned into five regions or windows by cutting small incisions using a laser into the bovine enamel blocks. The incision area also has an increased resistance to acid dissolution that serves to more effectively isolate each group[9]. Incisions were etched using a transverse excited atmospheric pressure (TEA) CO_2 laser operating at 9.3-μm, Impact 2500, GSI Lumonics (Rugby, UK). A thin layer of acid resistant varnish in the form of red nail polish, Revlon (New York, NY) was applied to protect the sound enamel control area before exposure to the 4.8 pH demineralization solution composed of a 40-mL aliquot of 2.0 mmol/L calcium, 2.0 mmol/L phosphate, and 0.075 mol/L acetate. Each sample was then placed into the demineralization solution and incubated at 37ºC. After each 24 hour period of demineralization, one region of each sample was covered with a thin layer of the same acid resistant varnish to prevent further demineralization. After the fourth day, the samples were removed from the demineralization solution and had all acid resistant varnish was removed using acetone. Each sample was then stored in 0.1% thymol solution to prevent fungal and bacterial growth.

2.2 PS-OCT System

A single-mode fiber autocorrelator-based Optical Coherence Domain Reflectometry (OCDR) system with polarization switching probe, high efficiency piezoelectric fiber-stretchers and two balanced InGaAs receivers that was designed and fabricated by Optiphase, Inc. (Van Nuys, CA) was integrated with a broadband high power superluminescent diode (SLD), Denselight (Jessup, MD) with an output power of 45-mW and a bandwidth of 35 nm and a high-speed XY-scanning system, ESP 300 controller & 850-HS stages, Newport (Irvine, CA) and used for *in vitro* optical tomography. The system was configured to provide an axial resolution at 22-μm in air and 14-μm in enamel and a lateral resolution of approximately 50- μm over the depth of foucs of 10 mm. The all-fiber OCDR system has been previously described in greater detail[10,11]. The PS-OCT system was completely controlled using LabVIEW™ software, National Instruments (Austin TX).

2.3 Polarized Light Microscopy (PLM) and Digital Transverse Microradiography (TMR)

After sample imaging was completed, approximately 200 μm thick serial sections were acquired using an Isomet 5000 saw (Buehler, IL), for polarized light microscopy (PLM) and digital transverse microradiography (TMR). PLM was carried out using a Meiji Techno RZT microscope (Meiji Techno Co., LTD, Saitama, Japan) with an integrated digital camera, Canon EOS Digital Rebel XT (Canon Inc., Tokyo, Japan). The sample sections were imbibed in water and examined in the brightfield mode with crossed polarizers and a red I plate with 500 nm retardation. A custom-built digital transverse microradiography (TMR) system was used to measure mineral loss in the different partitions of the sample. A high-speed motion control system with Newport UTM150 and 850G stages and an ESP300 controller coupled to a video microscopy and laser targeting system was used for precise positioning of the tooth samples in the field of view of the imaging system. The volume

percent mineral for each sample thin section was determined by comparison with a calibration curve of x-ray intensity versus sample thickness created using sound enamel sections of 86.3 ± 1.9% volume percent mineral varying from 50 to 300 μm in thickness. The calibration curve was validated via comparison with cross sectional microhardness measurements. The volume percent mineral determined using microradiography for section thickness ranging from 50 to 300 μm highly correlated with the volume percent mineral determined using microhardness $r^2 = 0.99$ (See paper #7162-33 in this proceedings).

2.4 Integrated Reflectivity

The integrated reflectivity was calculated in each of the five windows (one sound, four demineralized) for every sample. Line profiles were taken from the orthogonal polarization (⊥-axis) PS-OCT images or b-scans in each of the five regions, and the reflectivity was integrated from the enamel surface to various depths, yielding the integrated reflectivity, ΔR, of the regions in units of decibels per micron. Previous studies have shown that ΔR correlates directly with the integrated mineral loss (volume % mineral × microns) called ΔZ [12,13].

2.5 Scan preparation

Figure 1 contains a diagram of the steps involved in the automated integration of the lesion areas. The Java programming language from Sun Microsystems, Inc. (Santa Clara, CA) was used, and each scan had background noise removed by subtracting the mean reflectivity of the scan from every position in the scan. If an encountered value during the removal of background noise was less than the mean reflectivity, the new value was set to zero. The background-subtracted scan was then converted into an 8-bit grayscale image where each pixel in the image was mapped to a corresponding reflectivity value obtained in the background-subtracted scan. For this experiment, a reflectivity threshold was selected consisting of the mean plus four times standard deviation. The mean and the standard deviation were computed from the background-subtracted scan using through the use of the Apache Commons Mathematics Library from the Apache Software Foundation (Forest Hill, MD). Figure 2a-b shows images produced from applying techniques discussed in this section.

2.6 Automated Calculation of Lesion Depth and Severity through Edge Finding

The range of line profiles to use for each window was selected manually by selecting lines between the laser-etched fiducial lines. The range of reflectivity values used in ΔR calculation from each line profile was determined using two different approaches: fixed-depth, and edge-detected [14]. Regardless of the approach, each approach establishes a method to determine the enamel surface boundary and a lesion depth boundary.

2.6.1 Fixed Depth—In the fixed-depth approach, the enamel surface boundary was determined by the intersection of the line profile and a manually established straight line that marks the enamel surface in a scan. The lesion boundary was set to an arbitrary depth of 200-μm from the established enamel line [7].

2.6.2. Edge Detected—In the edge-detected approach, the enamel edge and the lesion boundary were selected in a three-step process. The first step was applying a 3x3 median

filter (Java Image Filters, JH Labs) to remove speckle noise. An adapted iterative anisotropic diffusion filter[15,16] with (iterations=30, K=10000, λ =0.05) was applied such that features (e.g. lesions) would be accented in the image. Finally, an edge locator would make two passes along each line—each pass starting from each end of the line—finding the first pixel whose color components all exceed e^{-2}. The distance between those positions represented the calculated depth of the lesion along that particular line. Figure 2c-e shows examples of the images produced in this approach.

3. RESULTS AND DISCUSSION

The fixed depth approach was not only able to distinguish between sound and demineralized enamel, but also able to distinguish between lesions created with varying periods of demineralization exposure as can be seen in Fig. 2. The edge-detected approach was also able to distinguish between sound and lesioned enamel while discriminating between lesions of various demineralization exposures. This approach was able to isolate a lesion with a depth of at least 40-μm and differentiate between two lesions with a depth difference of at least 3-μm. After scanning with PS-OCT the bovine samples were cut into sections approximately 200-μm thick and examined with polarized light microscopy and microradiography. Fig. 3 shows a low magnification PLM image of one of the thin sections which shows the lesion progression after each period. The left and right sides of the sample are sound and the lesion severity increases from the left to the right with a similar depth to that measured using PS-OCT. Demineralization is inhibited in the incision areas due to heating by the CO_2 laser.

This study demonstrates that edge detection algorithms can be used to identify lesion areas on OCT scans for the automated processing of PS-OCT images. In previous PS-OCT studies, the severity of lesion areas was accessed by integration of single a-scans. Better discrimination of lesion areas is possible if the entire lesion cross-section area or volume is integrated as opposed to a single a-scan. This is only feasible with algorithms for automated processing.This becomes even more important for the efficient implementation of FD-OCT systems that are capable of the acquisition of entire lesion volumes, e.g., $2 \times 2 \times 3$ mm^3 volumes, at video rates. Two approaches were investigated, namely edge detection was used to identify the enamel surface and the lesion was integrated to a fixed depth and the edge detection was used to identify both the enamel surface and the lesion depth. Both approaches enable discrimination between different intervals of demineralization. The PS-OCT system employed in this study utilized an autocorrelator with single-mode fiber along with a electromagnetic Faraday switch to acquire each polarization state. This system was used because it yields very clean PS-OCT images free of artifacts. One disadvantage in using a PS-OCT system with polarization maintaining fiber is that images from such systems typically have artifacts in the images. Such artifacts would likely prevent successful implementation of this approach. Therefore it is necessary to use a very “clean” PS-OCT system in order for this approach to work. Statistical comparisons of the PS-OCT scans, PLM images and Microradiographic scans for all the samples will be submitted for publication in a future article to be submitted for publication in the future.

Acknowledgments

The authors acknowledge the support of NIH grants R01-DE017869 and R01-DE14698.

4. REFERENCES

1. NIH. Report No. 18. 2001. Diagnosis and Management of Dental Caries throughout Life.
2. Baumgartner A, Hitzenberger CK, Dicht S, Sattmann H, Moritz A, Sperr W, Fercher AF. Optical coherence tomography for dental structures. Lasers in Dentistry IV, San Jose. 1998; 3248:130–136.
3. Dicht S, Baumgartner A, Hitzenberger CK, Sattmann H, Robi B, Moritz A, Sperr W, Fercher AF. Polarization-sensitive optical optical coherence tomography of dental structures. Lasers in Dentistry V, San Jose. 1999; 3593:169–176.
4. Baumgartner A, Dicht S, Hitzenberger CK, Sattmann H, Robi B, Moritz A, Sperr W, Fercher AF. Polarization-sensitive optical optical coherence tomography of dental structures. Caries Res. 2000; 34:59–69. [PubMed: 10601786]
5. Everett MJ, Colston BW, Sathyam US, Silva LBD, Fried D, Featherstone JDB. Non-invasive diagnosis of early caries with polarization sensitive optical coherence tomography (PS-OCT). Lasers in Dentistry V, San Jose. 1999; 3593:177–183.
6. Wang XJ, Zhang JY, Milner TE, Boer JFd, Zhang Y, Pashley DH, Nelson JS. Characterization of Dentin and Enamel by use of Optical Coherence Tomography. Appl Opt. 1999; 38:586–590.
7. Fried D, Xie J, Shafi S, Featherstone JDB, Breunig T, Lee CQ. Early detection of dental caries and lesion progression with polarization sensitive optical coherence tomography. J Biomed Optics. 2002; 7:618–627.
8. Darling CL, Huynh GD, Fried D. Light Scattering Properties of Natural and Artificially Demineralized Dental Enamel at 1310-nm. J Biomed Optics. 2006; 11:034023, 034021-034011 .
9. Can AM, Darling CL, Ho CM, Fried D. Non-destructive Assessment of Inhibition of Demineralization in Dental Enamel Irradiated by a λ=9.3-μm CO_2 Laser at Ablative Irradiation Intensities with PS-OCT. Lasers in Surgery and Medicine. 2008; 40:342–349. [PubMed: 18563781]
10. Bush J, Davis P, Marcus MA. All-Fiber Optic Coherence Domain Interferometric Techniques. Fiber Optic Sensor Technology II. 2000; 4204:71–80.
11. Ngaotheppitak P, Darling CL, Fried D, Bush J, Bell S. PS-OCT of occlusal and interproximal caries lesions viewed from occlusal surfaces. Lasers in Dentistry X. 2006; 6137:61370L.
12. Jones RS, Darling CL, Featherstone JDB, Fried D. Imaging artificial caries on occlusal surfaces with polarization sensitive optical coherence tomography. Caries Res. 2004; 40:81–89. [PubMed: 16508263]
13. Ngaotheppitak P, Darling CL, Fried D. Polarization Optical Coherence Tomography for the Measuring the Severity of Caries Lesions. Lasers Surg Med. 2005; 37:78–88. [PubMed: 15889402]
14. Nixon, MS.; Aguado, AS. Feature Extraction and Image Processing. 2. Academic Press; Boston: 2004.
15. Perona P, Malik J. Scale-Space and Edge Detection using Anisotropic Diffusion. IEEE Trans PAMI. 1990; 17:629–639.
16. Otsu N. A Threshold Selection Method from Gray-Level Histograms. A Threshold Selection Method from Gray-Level Histograms. IEEE Trans SMC. 1979; 9:62–66.

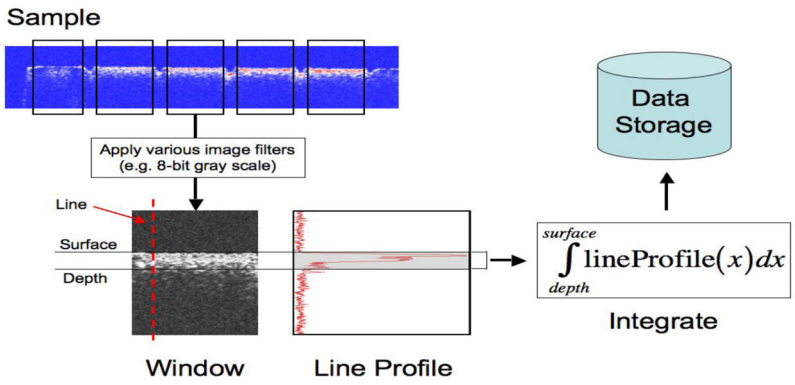

Fig. 1.
Diagrammatical representation of the automatic algorithm used in this experiment.

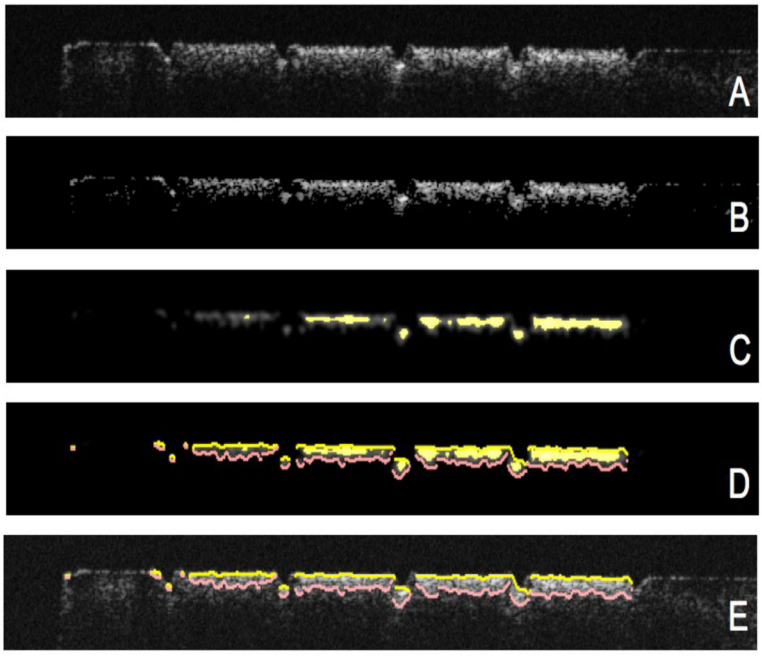

Fig. 2.

(A) A gray-scale converted OCT b-scan (B) Image adjusted with a threshold filter (C) Image after anisotropic diffusion, a filtration process designed to locate features (D) Edges located using an edge locator function (E) Found edges of D overlaid on A.

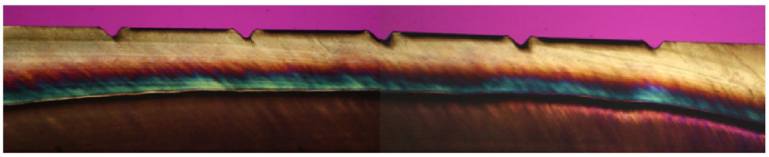

Fig. 3.

Polarized light image of one of the samples after four days of demineralization. Sound regions are on the ends of the sample and each 1-day interval of demineralization is shown with increasing severity from the left to the right.